

Inter-seasonal comparison of acoustic propagation in a *Thalassia testudinum* seagrass meadow in a shallow sub-tropical lagoon

Cite as: JASA Express Lett. **3**, 010801 (2023); <https://doi.org/10.1121/10.0016752>

Submitted: 06 September 2022 • Accepted: 12 December 2022 • Published Online: 04 January 2023

 Kevin M. Lee,  Megan S. Ballard,  Andrew R. McNeese, et al.

COLLECTIONS

 This paper was selected as an Editor's Pick



View Online



Export Citation

ARTICLES YOU MAY BE INTERESTED IN

[Impacts of seafloor characteristics on three-dimensional sound propagation in a submarine canyon](#)

JASA Express Letters **3**, 016002 (2023); <https://doi.org/10.1121/10.0016835>

[Range estimation of a moving source using interference patterns in deep water](#)

JASA Express Letters **2**, 126001 (2022); <https://doi.org/10.1121/10.0016402>

[Using transfer learning with a convolutional neural network to detect African manatee \(*Trichechus senegalensis*\) vocalizations](#)

JASA Express Letters **2**, 121201 (2022); <https://doi.org/10.1121/10.0016543>



Advance your science and career
as a member of the
[ACOUSTICAL SOCIETY OF AMERICA](#)

LEARN MORE 

Inter-seasonal comparison of acoustic propagation in a *Thalassia testudinum* seagrass meadow in a shallow sub-tropical lagoon

Kevin M. Lee,^{1,a)}  Megan S. Ballard,¹  Andrew R. McNeese,¹  Preston S. Wilson,^{2,a)}  Gabriel R. Venegas,^{1,b)}  Mathew C. Zeh,^{2,c)}  and Abdullah F. Rahman³

¹Applied Research Laboratories, The University of Texas at Austin, Austin, Texas 78713, USA

²Walker Department of Mechanical Engineering, The University of Texas at Austin, Austin, Texas 78712, USA

³School of Earth, Environmental, and Marine Sciences, University of Texas Rio Grande Valley, Brownsville, Texas 78520, USA

kevin.lee@arlut.utexas.edu, meganb@arlut.utexas.edu, mcneese@arlut.utexas.edu, pswilson@mail.utexas.edu, g.venegas@unh.edu, matthew.zeh@belmont.edu, abdullah.rahman@utrgv.edu

Abstract: Acoustic propagation measurements were collected in a seagrass meadow in a shallow lagoon for periods of over 65 h in winter and 93 h in summer. A bottom-deployed sound source transmitted chirps (0.1–100 kHz) every 10 min that were received on a four-receiver horizontal hydrophone array. Oceanographic probes measured various environmental parameters. Daytime broadband acoustic attenuation was 2.4 dB greater in summer than winter, and the median received acoustic energy levels were 8.4 dB lower in summer compared to winter. These differences were attributed in part to seasonal changes in photosynthesis bubble production and above-ground seagrass biomass. © 2023 Author(s). All article content, except where otherwise noted, is licensed under a Creative Commons Attribution (CC BY) license (<http://creativecommons.org/licenses/by/4.0/>).

[Editor: David R. Barclay]

<https://doi.org/10.1121/10.0016752>

Received: 6 September 2022 Accepted: 12 December 2022 Published Online: 4 January 2023

1. Introduction

Seagrasses serve major global ecological roles in biodiversity and fisheries support, coastal protection, water filtration, nutrient cycling, and carbon sequestration.^{1,2} Furthermore, seagrasses have been proposed as a nature-based solution to help mitigate the effects of climate change.^{3,4} Current global estimates of seagrass coverage are uncertain,⁵ and seagrass decline rate estimates range from approximately 1%–7% per year, due in part to anthropogenic causes, such as coastal development, pollution, and destructive fishing practices.^{6,7} Therefore, developing improved methods to widely, accurately, and efficiently assess seagrass coverage and rates of decline are critical to promoting sustainable seagrass conservation efforts.

Seagrasses produce oxygen from photosynthesis. Gas bodies (lacunae) within the plant tissue exchange carbon dioxide and oxygen throughout the plant, keeping the leaves buoyant. Under high irradiance conditions, the partial pressure of oxygen contained in the lacunae exceeds that of the surrounding water, and oxygen diffuses through the plant tissue to form bubbles on the surfaces of the leaves. These bubbles are released from the leaves in a continuous stream during peak daylight hours of photosynthesis. Oxygen is also transferred continually to the sediment surrounding the rhizomes and roots due to generally hypoxic conditions in the sediment at varying rates based on photosynthesis and respiration. All these gas volumes have implications for underwater acoustic propagation where seagrass is present because bubbles in liquid, biological tissue, or sediment lead to acoustic dispersion, absorption, and scattering.^{8–10}

The use of underwater acoustics to remotely sense seagrass has been studied since the mid-1990s. Many previous efforts have employed high-frequency backscatter techniques to map seagrass coverage.¹¹ Another technique employs broadband acoustic propagation measurements in seagrass meadows to sense oxygen production by seagrass photosynthesis.^{12–17} In the latter, oxygen bubbles act as biophysical markers that can be exploited to infer seagrass productivity. Propagation experiments (0.1–16 kHz) in Mediterranean *Posidonia oceanica* demonstrated strong correlation between received acoustic energy level, with variations up to 5–6 dB, and water column oxygen bubble concentration, estimated from dissolved oxygen measurements.^{12–14} In these experiments, water depths ranged from 8–25 m, such that the seagrass, with leaves up to 0.5 m tall, filled a small fraction of the water column. Another propagation experiment (2–8 kHz) was

^{a)}Also at: Applied Research Laboratories, The University of Texas at Austin, Austin, TX 78713, USA. Author to whom correspondence should be addressed.

^{b)}Current address: Center for Acoustics Research and Education, University of New Hampshire, Durham, NH 03824, USA.

^{c)}Current address: Chemistry and Physics Department, Belmont University, Nashville, TN 37212, USA.

conducted in an extremely shallow water (0.3–0.8 m) with the tropical Indo-Pacific species *Cymodocea rotundata*.¹⁵ Here, the seagrass filled a much greater fraction of the water column. Sound pressure level variation of 40 dB over a diurnal cycle was reported in this study; however, it was noted that the changing water depth due to tides influenced the observed signal level variation. Another study examined differences in broadband propagation (0.1–100 kHz) between a densely vegetated *Thalassia testudinum* meadow and a nearby sparsely vegetated area with otherwise similar waveguide characteristics (1–1.5 m water depth).¹⁶ Here, it was found that received acoustic energy levels were lower in the densely vs sparsely vegetated areas by nearly 30 dB, indicating that acoustic propagation was sensitive to the amount of seagrass present, in addition to the photosynthesis bubbles. Most of these previous seagrass meadow acoustic propagation experiments lasted from one to a few consecutive days, either in a single season^{13–16} or at different times of year with similar environmental conditions.¹² This letter reports a long-term seagrass acoustic propagation experiment in the same *T. testudinum* meadow as the latter study, in which measurements were collected in winter and summer at a fixed location to examine the sensitivity of acoustic propagation to seasonal changes in photosynthesis oxygen bubble production and the amount of above-ground seagrass biomass.

2. Description of experiment

The experiment was conducted in a seagrass meadow in the Lower Laguna Madre, part of a shallow hypersaline lagoon system on the southern Texas Gulf of Mexico coast (Fig. 1). The seagrass meadows of the Lower Laguna Madre are the largest on the Texas coast and are representative of the Tropical Atlantic seagrass bioregion.¹⁸ The dominant seagrass species is *T. testudinum* although smaller abundances of *Halodule wrightii* and *Syringodium filiforme* are also present throughout the lagoon. *T. testudinum* leaf and rhizome production rates exhibit seasonal patterns, and below-ground biomass accounts for 80%–90% of the total biomass.^{19–22} There is a strong seasonal dependence of the above-ground biomass, in which above-ground biomass and leaf production are at a minimum in the winter months and peak in the summer months. Below-ground biomass has less seasonal dependence, being more constant throughout the year. The measurements were conducted during 11–14 February 2019 and 17–20 September 2019 to sample this seasonal dependence. The measurement site ($26^{\circ} 6.556' N$, $97^{\circ} 10.422' W$) was located approximately 175 m from shore.

An omnidirectional spherical piezoelectric sound source (10 cm diameter) and four cylindrical hydrophone receivers (3.8 cm long, 3 cm diameter) were deployed at the measurement site. The centers of the source and hydrophones were positioned approximately 20 cm and 10 cm above the lagoon floor, respectively, and separated by horizontal distances of 1.5, 3, 6, and 12 m (Fig. 1). The transducer layout was chosen based on previous work by the authors in the Lower Laguna Madre seagrass meadow conducted in October 2018.¹⁶ In this previous work, good signal-to-noise ratio was observed at 6 m source/receiver separation distance. In an effort to extend the propagation range in the current study while maintaining good signal level, the receiver at 12 m was added. The water depth at the site fluctuated between approximately 0.6–1.2 m due to changing tide, thus the propagation distance was several water depths for the greatest source/receiver separation distance. The seagrass canopy height ranged from approximately 5–10 cm in February to greater than 30 cm in September, such that the source and hydrophones were either mostly exposed to the water column in winter or partially obscured by seagrass leaves in summer. The transducers were not continuously deployed throughout the year; rather, the authors deployed and recovered the equipment in February and then returned to the same site in September and replicated the transducer layout. The transducers were cabled to shore, where signal generation and data acquisition electronics were stationed, allowing for continuous monitoring of the experiment during the two measurement campaigns. Source transmission events were scheduled to repeat every 10 min over the duration of the experiment for 144 transmissions per day. For each transmission event, 10 chirps were broadcast every 2 s and then averaged. The source excitation

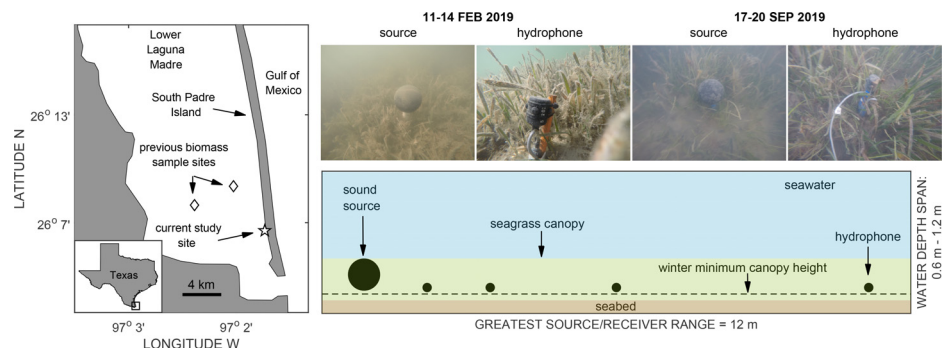


Fig. 1. Map displays the location of the experiment in the Lower Laguna Madre. The current study site and previous seagrass biomass sampling sites are indicated. Photographs show the difference in seagrass coverage at the experiment site between the two seasons. The measurement configuration is shown in the diagram, with hydrophones located at distances of 1.5, 3, 6, and 12 m from the sound source.

exponential chirp waveform (0.1–100 kHz bandwidth, 50 ms duration) and pulse compression signal processing used to obtain the band limited, waveguide impulse response are described in Ref. 16.

The total received acoustic energy,¹³ which is inclusive of all multi-path arrivals at the receiver, was computed at each receiver for each transmission event:

$$\mathcal{E} = \int_T h(t)^2 dt, \quad (1)$$

where $h(t)$ is the band limited waveguide impulse response and T is a time interval that encompasses the received signal, which had a long, reverberant tail. For the numerical integration, a window length of 30 ms was used. Increasing the window length had very little effect on the resultant value; hence, most of the signal energy was included in this window. The total acoustic energy level in decibels for each receiver is defined as

$$E = 10 \log_{10} \left[\frac{\mathcal{E}}{\mathcal{E}_0} \right], \quad (2)$$

where \mathcal{E}_0 is a reference energy, which is defined here as the median total acoustic energy measured on the closest receiver in February. Broadband waveguide attenuation α was estimated from a linear least squares fit to the natural logarithm of total received acoustic energy as a function of source/receiver separation distance R with the fit having the functional form

$$\ln \mathcal{E} = \mathcal{E}' - \alpha R, \quad (3)$$

where \mathcal{E}' is a constant. Attenuation was computed from energy measured on receivers at 1.5, 3, and 6 m because the signal on the 12 m receiver was noise-limited during the final daytime cycles in September.

Autonomous sensor-equipped data loggers were deployed on the lagoon floor adjacent to the source to acquire time records of dissolved oxygen, water temperature, water depth, and salinity in 5 min intervals. A blackbody thermopile pyranometer was mounted near the on-shore station in a location that remained unshaded by nearby structures throughout the day to measure solar irradiance every 5 min. Nearby weather station PCGT2, operated by the Texas Coastal Ocean Observing Network, provided wind speed and direction data in 4 min intervals.²³

3. Results

Time records of the environmental parameters and acoustic data reveal complex temporal dependence influenced by diurnal and seasonal patterns as well as transient weather events (Fig. 2). A weather system associated with a seasonal cold front and storms passed through the region at the beginning of the February experiment, evident from high and variable wind speed and wind direction from the north, affecting the water conditions in the lagoon. During this period, there was also significant cloud cover leading to a decrease in solar irradiance. Dissolved oxygen was close to 100% saturation, resulting from a combination of air entrainment by waves and rain as well as daytime oxygen produced by the seagrass from photosynthesis. Dissolved oxygen itself is expected to have very little effect on the acoustic propagation; rather, it is a proxy measurement for bubbles in the water column. During this initial period, the acoustic propagation was likely influenced by weather-induced bubble entrainment and water surface roughness, as indicated by variable total acoustic energy levels, spectral levels, and attenuation. After the frontal weather system passed, conditions were more quiescent, and the winter diurnal pattern emerged. During the day on 13 February 2019, oxygen production from seagrass photosynthesis leads to higher rates of bubble formation and release into the water column, resulting in a 4.3 dB/m increase in attenuation compared to night and reduction in spectral levels in the approximately 1–3 kHz band. It is expected that the frequency dependence of the received signals, and hence the attenuation, depends upon the bubble size distribution although this was not characterized.

The September data displayed a regular diurnal pattern over the entire 4-day measurement period (Fig. 2). Dissolved oxygen level excursions had greater extrema than the February data from the quiescent period, with nighttime minima less than 50% saturation and daytime maxima approaching 200% saturation, indicative of higher photosynthesis bubble production in the summer. The night-day difference in received attenuation ranged from approximately 4.6 dB/m at the start of the September measurements to nearly 6.7 dB/m at the end of the week. During the first 2 days of this time period, the spectral levels displayed reduction at frequencies higher than 9 kHz, which coincided with periods of increased bubble production, indicated by the dissolved oxygen maxima. In the final 2 days of the experiment, when highest attenuation was observed, the bandwidth of the spectral level reduction increased with significant reduction across most of the band. During this period, the water depth was at its lowest at times coincident with the highest bubble production (indicated by the dissolved oxygen maxima). This low tide caused the volume fraction of the seagrass leaves, and hence lacunae, in the water column to increase, which likely enhanced the attenuation.

Pearson correlation coefficients r and p -values were calculated between the attenuation and the various environmental parameters. The September attenuation had strong negative correlation with dissolved oxygen ($r = 0.8, p < 0.001$), indicative of the relationship between photosynthesis-driven bubble production by the seagrass and increased attenuation in the waveguide. Because the bubble production is driven by sunlight, there was also a strong correlation between solar

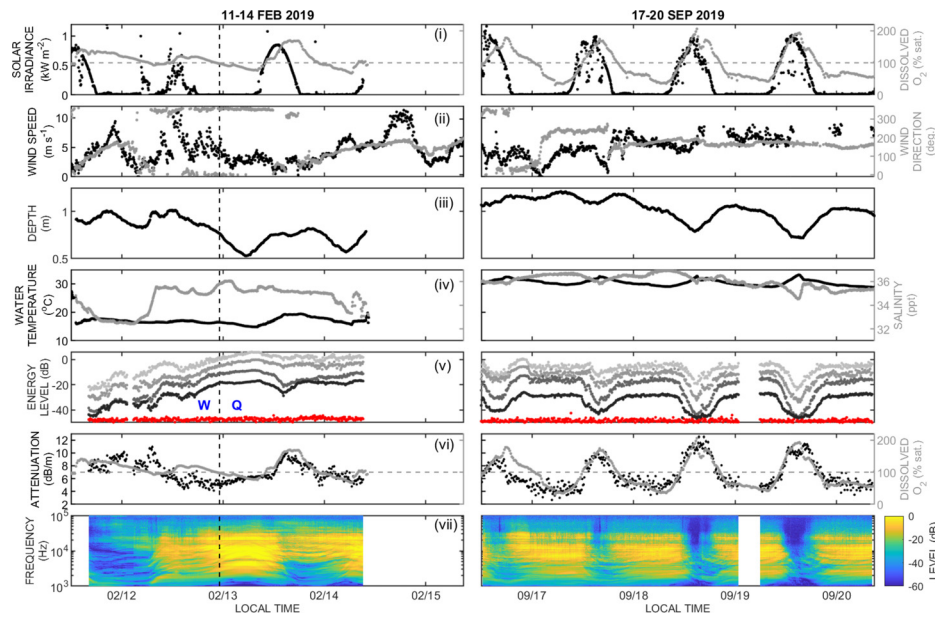


Fig. 2. Time series of measured environmental and acoustic quantities in February and September are shown. Total acoustic energy levels [row (v)], from Eq. (2) are relative to the median February level at the closest receiver, which is defined as 0 dB here. Energy levels on the closest to farthest receivers are rendered from light to dark gray. Ambient noise levels (post-pulse compression) are shown in red. Attenuation [row (vi)] was computed from energy measured on receivers at 1.5, 3, and 6 m because the signal on the 12 m receiver was noise-limited during the final daytime cycles in September. Spectrograms from the 6 m hydrophone data [row (vii)] are relative to the maximum February spectral level, and the decrease in spectral levels above 30 kHz is due to the frequency response of the transducers. The vertical dashed line in the February column indicates the approximate boundary between weather-dominated (W) and quiescent (Q) conditions. The horizontal dashed line in rows (i) and (vi) indicates dissolved oxygen level of 100% saturation. The gap in acoustic data during the September measurement period was caused by an unintended computer restart in the middle of the night, resulting in a data dropout between 00:47 and 05:55 on 19 September 2019. The total duration of time shown on the horizontal scales for each column are the same (93 h) to facilitate comparison between data from the two measurement campaigns.

irradiance and attenuation ($r = 0.7, p < 0.001$). The water temperature exhibited a diurnal pattern due to solar heating; therefore, there was positive correlation between attenuation and water temperature ($r = 0.7, p < 0.001$). Negative correlation between attenuation and water depth ($r = -0.6, p < 0.001$) was influenced by the tidal pattern being roughly synchronized with the diurnal pattern, particularly during the latter portion of the week. When water was shallowest, the lacunae occupied a larger fraction of the water column. Due to the timing, this occurred when the bubble production was also greatest, and the sound attenuating effects of each were reinforced. Finally, there was no significant correlation ($|r| < 0.3$) between attenuation and salinity or wind speed in September. Correlation coefficients between attenuation and environmental parameters for the entire February dataset reflected less obvious influence from diurnal patterns, which is expected given that the weather event dominated half the measurement period. Therefore, the February data were split into two segments for the correlation analysis—weather-dominated and quiescent periods. During the quiescent period, the attenuation had the strongest correlation with dissolved oxygen ($r = 0.8, p < 0.001$) and was similar in magnitude to the September dataset. There was also significant correlation between attenuation and water temperature ($r = 0.8, p < 0.001$), and modest positive correlation with solar irradiance and water depth ($r = 0.5, p < 0.001$). Correlation coefficients in this period between attenuation and wind speed and salinity were low ($|r| < 0.5$). In the weather-dominated portion of the February dataset, the attenuation had the highest correlation with salinity ($r = -0.7, p < 0.001$). A marked decrease in salinity occurred during the weather event, from 34.8–32.5 ppt, followed by a quick rise to 35.5 ppt. This rise coincided with a decrease in attenuation, giving rise to the negative correlation. Correlations between attenuation and all other environmental parameters were low in the weather-dominated period ($|r| < 0.3$).

Correlations between environmental parameters were also examined to assess which parameters were independent of one another and whether photosynthesis was a primary driver of temporal changes in the attenuation. Dissolved oxygen was correlated to solar irradiance in September ($r = 0.7, p < 0.001$) and the February quiescent period ($r = 0.5, p < 0.001$) due to the relationship between sunlight and photosynthesis bubble production, but dissolved oxygen and irradiance had virtually no correlation in the February weather-dominated period. Dissolved oxygen and water temperature had high correlation in all three measurement periods ($r = 0.9, p < 0.001$) because the capacity of water to dissolve oxygen is temperature dependent. Modest correlation ($r = 0.5, p < 0.001$) between water depth and salinity was observed in September when the prevailing wind direction was mostly from the south (Fig. 2), potentially indicating seawater flow

from the southern to northern Gulf inlets to the lagoon. No significant correlation ($|r| < 0.3$) between water depth and salinity was observed in weather-dominated or quiescent periods in February. No significant correlation was observed between water depth and dissolved oxygen, irradiance, or temperature during the September measurement period or the February weather-dominated period. In the February quiescent period, water depth was correlated to dissolved oxygen ($r = 0.7, p < 0.001$) and temperature ($r = 0.8, p < 0.001$). Finally, in the weather-dominated February period, salinity exhibited negative correlation with dissolved oxygen ($r = -0.6, p < 0.001$) and water temperature ($r = -0.5, p < 0.001$). The decrease in salinity during this period coincided with the cold front and associated rain, which likely resulted in lower temperature and elevated dissolved oxygen from bubble entrainment.

4. Comparison with previous biomass estimates

Previous estimates of above-ground seagrass biomass from nearby sampling sites were compared with total acoustic energy levels from the present study (Fig. 3). While biomass measurements were not collected as part of the current study, measurements were previously collected by Kaldy and Dunton¹⁹ at two sites approximately 5 and 7 km away from the current measurement site (Fig. 1). Although these measurements were collected in 1995–1996, the relative seasonal changes are representative for *T. testudinum* in this coastal region and others in the Tropical Atlantic bioregion.^{20–22} Whereas there was no seasonal pattern in below-ground biomass established in the previous study, above-ground biomass exhibited a seasonal dependence. Estimates of above-ground biomass per unit area were $75.5 \pm 26.7 \text{ gdw m}^{-2}$ in February and $120.0 \pm 30.9 \text{ gdw m}^{-2}$ in September (mean \pm st. dev.), indicating that the canopy was expected to be taller and have more shoots in September compared to February. These measurements were compared with distributions of total acoustic energy level measured on the 12 m receiver because this represents the longest propagation path and hence, the most interaction with the seagrass leaves and lacunae. The median total acoustic energy level in September was 8.4 dB lower than the level in February. The distributions were skewed to lower energy events resulting from either photosynthesis bubble production, tidal influence, the storm event that occurred during the February measurement period, or combinations of these. Comparing the median value over the entire measurement period filters out these shorter lived, lower energy events, thus, the median total acoustic energy represents a potential acoustic measure of the background state of the propagation waveguide.

5. Discussion

Differences in the attenuation were examined between both day/night and the two seasons. During the quiescent portion of the February measurement period, there was a 4.3 dB increase in the daytime attenuation relative to nighttime levels. Attenuation during this period had high correlation with dissolved oxygen and irradiance and modest positive correlation with water depth. In September, as much as a 6.7 dB increase in daytime attenuation relative to nighttime levels was observed with high positive correlation with dissolved oxygen and irradiance and negative correlation with water depth. The day/night attenuation difference was increased in September compared to February. This was in part due to increased bubble production by the seagrass in September (relative to February) when there is higher irradiance and temperature, which are conditions more favorable for the seagrass to produce bubbles. Additionally, *T. testudinum* above-ground biomass and leaf growth is known to have seasonal dependence, not only in the meadow in this study¹⁹ but also in other *T. testudinum* meadows within the same bioregion.^{20–22} With taller leaves and denser growth in the summer months, the seagrass canopy fills more of the water column, meaning there is more leaf surface area for attached bubbles and a greater volume fraction of lacunae in the waveguide. Comparing day/night attenuation in a single season indicates differences in

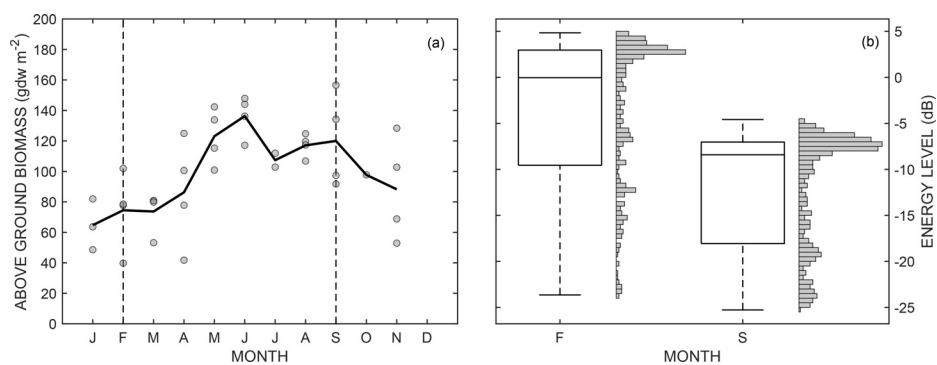


Fig. 3. (a) Above-ground seagrass biomass data from Kaldy and Dunton,¹⁹ collected in 1995 and 1996. The data are represented by circles, and the solid line indicates the mean. (b) Distributions of total acoustic energy level measured at the 12 m receiver calculated using Eq. (2) for February ($N = 383$) and September ($N = 524$) from the present study. The distributions are plotted at histograms. The distributions are relative to the February median (shown as zero on this figure).

free bubbles (on leaves and in water column) from photosynthesis, assuming the lacunae fill approximately the same volume fraction. Tidal change in water depth also factors into the attenuation because this affects the volume fractions of free bubbles and lacunae in the waveguide. When the tides are approximately synchronized with the diurnal cycle, there can be increased bubble production from photosynthesis at the same time the waveguide has a higher fraction of lacunae leaves leading to higher attenuation than from either component on its own. When the tide and diurnal cycle are not aligned, the combined effects could be less pronounced. An example of this difference can be observed by comparing the first two and last two daytime periods of diurnal cycles in the September dataset. When low tide is synchronized with the diurnal cycle (last 2 days), the attenuation is higher than when the tide is high during daylight hours (first 2 days). This difference in daytime attenuation is attributed to the waveguide having a higher volume fraction of lacunae at low tide, as the photosynthesis bubble production rates are presumably similar between the two times.

Distributions of total received acoustic energy level at the 12 m receiver were compared with previous estimates of above-ground seagrass biomass in the lagoon. Above-ground seagrass biomass itself is not expected to have direct significant effects on the propagation, but the lacunae contained within the biomass do influence the propagation. The September median total acoustic energy level was 8.4 dB lower than the median level in February. This decrease in level is likely due to both the seasonal increase in volume fraction of lacunae within the waveguide and differences in photosynthesis bubble production. The below-ground seagrass biomass, which is representative of the roots and rhizomes, was not directly addressed here. Previous seasonal biomass estimates indicate that below-ground biomass is relatively constant throughout the year, even though the above-ground portions of the plants tend to go dormant in the winter.¹⁹ Therefore, the below-ground portions of the plants, which also contain lacunae, are assumed to have a relatively constant effect on the acoustic propagation throughout the year. The above-ground biomass is expected to have a much greater effect on acoustic propagation than the below-ground biomass.

Aspects of the present experiment could be improved in future campaigns. First, the frequency dependence of the attenuation is related to the bubble size distribution, which includes rising bubbles in the water column, bubbles attached to the leaves, and lacunae. No attempt was made to quantify the bubble size distribution in the water and on the leaves although this could be accomplished using a suitable *in situ* optical camera setup, given the water clarity at the site. Whereas optical methods would not work for quantifying the size distribution of the lacunae, samples of the leaves could be separated from the plants and imaged later in the laboratory with X-ray computed tomography¹⁷ or other methods. Second, no attempt was made to quantify stratification of the shallow water column. Salinity and temperature measurements were made at single location in proximity to the lagoon floor, but several measurement points spanning the water column would establish where stratification was present or not and whether refraction could be eliminated as a mechanism contributing to the attenuation. Third, although an attempt was made to infer information about currents in the lagoon from correlation between depth and salinity measurements, a current sensor could be deployed to directly measure water flow, which could affect how tall the seagrass leaves stand in the water column and potentially impact the propagation. Finally, data from only a few diurnal cycles were analyzed. More robust correlation would be supported by data over a larger number of cycles.

6. Conclusion and future work

This letter reports *in situ* acoustic propagation measurements in a *T. testudinum* meadow over several diurnal cycles both in late winter and summer. The received acoustic energy and attenuation were sensitive to temporal changes both in photosynthesis bubble production and lacunae in the above-ground seagrass biomass. Daytime attenuation increase relative to night was 4.3 dB in February and 6.7 dB in September. This day/night attenuation difference was primarily higher in the summer due to increased photosynthesis bubble production although tidal changes in water depth also contributed by varying the volume fraction of lacunae in the waveguide. The median total acoustic energy level in September was 8.4 dB lower than the median level in February. This decrease was attributed to seasonal increases in volume fraction of lacunae within the waveguide and photosynthesis bubble production. Future work will examine measurements over an entire year or longer. These measurements will reduce the relative importance of transient weather events, like the one observed in the February measurement period, allowing for nearly continuous monitoring of long-term changes in seagrass productivity and biomass. Furthermore, measurements of above- and below-ground biomass will be performed at the same time and place as the acoustic measurements in future studies to provide a more accurate and quantitative comparison.

Acknowledgments

This was supported by the Applied Research Laboratories Independent Research and Development program, National Science Foundation Grant No. 2023211, and United States Office of Naval Research Grant Nos. N00014-21-1-2254 and N00014-21-1-2245.

References and links

¹R. J. Orth, T. J. B. Carruthers, W. C. Dennison, C. M. Duarte, J. W. Fourqurean, K. L. Heck, Jr., A. R. Hughes, G. A. Kendrick, W. J. Kenworthy, S. Olyarnik, F. T. Short, M. Waycott, and S. L. Williams, "A global crisis for seagrass ecosystems," *BioScience* **56**, 987–996 (2006).

²J. W. Fourqurean, C. M. Duarte, H. Kennedy, N. Marbà, M. Holmer, M. A. Mateo, E. T. Apostolaki, G. A. Kendrick, D. Krause-Jensen, K. J. McGlathery, and O. Serrano, "Seagrass ecosystems as a globally significant carbon stock," *Nat. Geosci.* **5**, 505–509 (2012).

³P. I. Macreadie, M. D. Costa, T. B. Atwood, D. A. Friess, J. J. Kelleway, H. Kennedy, C. E. Lovelock, O. Serrano, and C. M. Duarte, "Blue carbon as a natural climate solution," *Nat. Rev. Earth Environ.* **2**, 826–839 (2021).

⁴R. Unsworth, L. C. Cullen-Unsworth, B. Jones, and R. J. Lilley, "The planetary role of seagrass conservation," *Science* **377**, 609–613 (2022).

⁵L. J. McKenzie, L. M. Nordlund, B. L. Jones, L. C. Cullen-Unsworth, C. Roelfsema, and R. K. Unsworth, "The global distribution of seagrass meadows," *Env. Res. Lett.* **15**, 074041 (2020).

⁶M. Waycott, C. M. Duarte, T. J. B. Carruthers, R. J. Orth, W. C. Dennison, S. Olyarnik, A. Calladine, J. W. Fourqurean, K. L. Heck, Jr., A. R. Hughes, G. A. Kendrick, W. J. Kenworthy, F. T. Short, and S. L. Williams, "Accelerating loss of seagrasses across the globe threatens coastal ecosystems," *Proc. Natl. Acad. Sci.* **106**, 12377–12381 (2009).

⁷J. C. Dunic, C. J. Brown, R. M. Connolly, M. P. Turschwell, and I. M. Côté, "Long-term declines and recovery of meadow area across the world's seagrass bioregions," *Glob. Change Biol.* **27**, 4096–4109 (2021).

⁸K. W. Commander and A. Prosperetti, "Linear pressure waves in bubbly liquids: Comparison between theory and experiments," *J. Acoust. Soc. Am.* **85**, 732–746 (1989).

⁹D. L. Miller, "A cylindrical-bubble model for the response of plant-tissue gas bodies to ultrasound," *J. Acoust. Soc. Am.* **65**, 1313–1321 (1979).

¹⁰H. Dogan, P. R. White, and T. G. Leighton, "Acoustic wave propagation in gassy porous marine sediments: The rheological and the elastic effects," *J. Acoust. Soc. Am.* **141**, 2277–2288 (2017).

¹¹M. U. Gümüşay, T. Bakırman, I. T. Kızılıkaya, and N. O. Aykut, "A review of seagrass detection, mapping, and monitoring applications using acoustic systems," *Eur. J. Remote Sens.* **52**, 1–29 (2019).

¹²J. P. Hermant, P. Nascetti, and F. Cinelli, "Inverse acoustical determination of photosynthetic oxygen productivity of posidonia seagrass," in *Experimental Acoustic Inversion Methods for Exploration of Shallow Water Environment* (Kluwer Academic, Netherlands, 2000), pp. 125–144.

¹³J. P. Hermant, "Acoustic remote sensing of photosynthetic activity in seagrass beds," in *Handbook of Scaling Methods in Aquatic Ecology: Measurement, Analysis, Simulation* (CRC Press, Boca Raton, FL, 2004), pp. 65–96.

¹⁴P. Felisberto, S. M. Jesus, F. Zabel, R. Santos, J. Silva, S. Gobert, S. Beer, M. Björk, S. Mazzuca, G. Procaccini, J. W. Runcie, and W. Champenois, "Acoustic monitoring of O₂ production of a seagrass meadow," *J. Exp. Mar. Biol. Ecol.* **464**, 75–87 (2015).

¹⁵A. Y. Y. Chang, L. Y. S. Chiu, M. H.-K. Mok, K. Soong, and W.-J. Huang, "Experimental observations of diurnal acoustic propagation effects in seagrass meadows on the Dongsha Atoll," *J. Acoust. Soc. Am.* **146**(3), EL279–EL285 (2019).

¹⁶K. M. Lee, M. S. Ballard, G. R. Venegas, J. D. Sagers, A. R. McNeese, J. R. Johnson, P. S. Wilson, and A. F. Rahman, "Broadband sound propagation in a seagrass meadow throughout a diurnal cycle," *J. Acoust. Soc. Am.* **146**, EL335–EL341 (2019).

¹⁷M. S. Ballard, K. M. Lee, J. D. Sagers, G. R. Venegas, A. R. McNeese, P. S. Wilson, and A. F. Rahman, "Application of acoustical remote sensing techniques for ecosystem monitoring of a seagrass meadow," *J. Acoust. Soc. Am.* **147**(3), 2002–2019 (2020).

¹⁸F. Short, T. Carruthers, W. Dennison, and M. Waycott, "Global seagrass distribution and diversity: A bioregional model," *J. Exp. Mar. Biol. Ecol.* **350**, 3–20 (2007).

¹⁹J. E. Kaldy and K. H. Dunton, "Above- and below-ground production, biomass, and reproductive ecology of *Thalassia testudinum* (turtle grass) in a subtropical coastal lagoon," *Mar. Ecol. Prog. Ser.* **193**, 271–283 (2000).

²⁰J. C. Zieman, "Seasonal variation of turtle grass, *Thalassia testudinum* König, with reference to temperature and salinity effects," *Aquat. Botany* **1**, 107–123 (1975).

²¹J. W. Fourqurean, A. Willsie, C. D. Rose, and L. M. Rutten, "Spatial and temporal pattern in seagrass community composition and productivity in south Florida," *Mar. Biol.* **138**, 341–354 (2001).

²²B. Martínez-Daranas, R. Cabrera, and F. Pina-Amargós, "Spatial and seasonal variability of *Thalassia testudinum* in Nuevitas Bay, Cuba," *J. Mar. Coast. Sci.* **1**, 9–27 (2009).

²³Information on the Station PCGT2 weather data archived by the U.S. National Buoy Data Center available at https://www.ndbc.noaa.gov/station_page.php?station=pcgt2 (Last viewed December 19, 2022).